

# Dynamics of Two Picophytoplankton Groups in Mediterranean Sea: Analysis of the Deep Chlorophyll Maximum by a Stochastic Advection-Reaction-Diffusion Model

Giovanni Denaro<sup>1</sup>, Davide Valenti<sup>1\*</sup>, Bernardo Spagnolo<sup>1\*</sup>, Gualtiero Basilone<sup>2</sup>, Salvatore Mazzola<sup>2</sup>, Salem W. Zgozi<sup>3</sup>, Salvatore Aronica<sup>2</sup>, Angelo Bonanno<sup>2\*</sup>

**1** Dipartimento di Fisica e Chimica, Università di Palermo, Group of Interdisciplinary Physics and Consorzio Nazionale Interuniversitario per le Scienze Fisiche della Materia, Unità di Palermo, Palermo, Italy, **2** Istituto per l'Ambiente Marino Costiero, Centro Nazionale delle Ricerche, Unità Operativa di Supporto di Capo Granitola, Campobello di Mazara, Trapani, Italy, **3** Marine Biology Research Centre, Tajura, Libya

## Abstract

A stochastic advection-reaction-diffusion model with terms of multiplicative white Gaussian noise, valid for weakly mixed waters, is studied to obtain the vertical stationary spatial distributions of two groups of picophytoplankton, i.e., picoeukaryotes and Prochlorococcus, which account about for 60% of total chlorophyll on average in Mediterranean Sea. By numerically solving the equations of the model, we analyze the one-dimensional spatio-temporal dynamics of the total picophytoplankton biomass and nutrient concentration along the water column at different depths. In particular, we integrate the equations over a time interval long enough, obtaining the steady spatial distributions for the cell concentrations of the two picophytoplankton groups. The results are converted into *chlorophyll a* and *divinil chlorophyll a* concentrations and compared with experimental data collected in two different sites of the Sicily Channel (southern Mediterranean Sea). The comparison shows that real distributions are well reproduced by theoretical profiles. Specifically, position, shape and magnitude of the theoretical deep chlorophyll maximum exhibit a good agreement with the experimental values.

**Citation:** Denaro G, Valenti D, Spagnolo B, Basilone G, Mazzola S, et al. (2013) Dynamics of Two Picophytoplankton Groups in Mediterranean Sea: Analysis of the Deep Chlorophyll Maximum by a Stochastic Advection-Reaction-Diffusion Model. PLoS ONE 8(6): e66765. doi:10.1371/journal.pone.0066765

**Editor:** Dante R. Chialvo, National Research & Technology Council, Argentina

**Received:** February 26, 2013; **Accepted:** May 13, 2013; **Published:** June 24, 2013

**Copyright:** © 2013 Denaro et al. This is an open-access article distributed under the terms of the Creative Commons Attribution License, which permits unrestricted use, distribution, and reproduction in any medium, provided the original author and source are credited.

**Funding:** The work was supported by the following: 1) Short visit grant, ref. n. 4933 within ESF Scientific Programme "Exploring the Physics of Small Devices (EPSD)", Unit PESC, coordinated by Prof. Christian Van den Broeck (<http://www.esf.org/activities/research-networking-programmes/physical-and-engineering-sciences-pesc/current-research-networking-programmes/exploring-the-physics-of-small-devices-epsd.html>); 2) Italian Ministry of University and Research (no specific grant) (<http://www.istruzione.it/>). The funders had no role in study design, data collection and analysis, decision to publish, or preparation of the manuscript.

**Competing Interests:** The authors have declared that no competing interests exist.

\* E-mail: [davide.valenti@unipa.it](mailto:davide.valenti@unipa.it) (DV); [bernardo.spagnolo@unipa.it](mailto:bernardo.spagnolo@unipa.it) (BS); [angelo.bonanno@iamc.cnr.it](mailto:angelo.bonanno@iamc.cnr.it) (AB)

## Introduction

The study of vertical profiles of phytoplankton in marine ecosystem is of fundamental importance to know the dynamics and structure of aquatic microorganisms [1–6]. In previous works, the distribution of phytoplankton in oceans and lakes have been obtained by using a deterministic approach to describe and reproduce the experimental data for the chlorophyll concentration. Two novelties are present in this work: i) the use of a stochastic approach to model the dynamics of more phytoplankton populations; ii) the comparison between theoretical and experimental distributions of chlorophyll concentration; this is performed by using, for each phytoplankton population, a conversion curve to obtain from the biomass concentrations the equivalent chlorophyll content. It is important to stress that marine ecosystems, because of the presence as well of non-linear interactions among their parts as deterministic and random perturbations due to environmental variables, are complex systems [7–23]. Therefore, in order to better reproduce this non-linear and noisy dynamics, it is necessary that the model takes into account

the presence of external random fluctuations [24,25] including, in the equations of our model, terms of multiplicative noise [14,26–28].

Phytoplankton is an essential component of all aquatic ecosystems in terms of biomass, diversity and production [29,30], and is responsible for a significant fraction of marine primary production [31,32]. The phytoplankton communities and their abundances depend on several phenomena of hydrological and biological origin, and involve different limiting factors [33]. The Mediterranean waters are generally characterized by oligotrophic conditions, and a previous work [34] has suggested that there is a decreasing trend over time in chlorophyll concentration in the Sicily Channel. This has been associated with increased nutrient limitation resulting from reduced vertical mixing due to a more stable stratification of the basin, in line with the general warming of the Mediterranean Sea [34–36].

It is worth noting that the production of fish species depends on the primary production of phytoplankton [30,37–39]. In general, the variations in the anchovy growth among different areas are mainly explained by changes in the chlorophyll concentration. In

particular, due to a decrease of biomass concentration in last years, we observed that the values of the anchovy growth in some regions of the Sicily Channel result to be in the low end of the range [40]. Therefore, this limited fish production could be a marker of low phytoplankton concentration, indicating a weak primary production in this area [59,68].

In this work we report on a study conducted in a hydrologically stable area of Mediterranean Sea, where the light intensity and nutrient concentration select different species and groups along water column, contributing to determine the biodiversity of the ecosystem. In fact, the growth of all phytoplankton groups is limited by the intensity of light  $I$  and concentration of nutrients  $R$  [2,5,6,41]. The light penetrates through the surface of the water and decreases exponentially along the water column. The nutrients, which are in solution, come from deeper layers of water column, near the seabed, and are characterized by an increasing trend from the surface waters to the benthic layer [2–4,28]. In Sicily Channel phosphorus, which is contained in phosphates present in solution, is the nutrient component playing the role of limiting factor for the growth of phytoplankton groups [42,43].

The responses of each picophytoplankton species to environmental solicitations strongly depend on the biological and physical parameters [5,44,45]. In particular, half-saturation constants determine the position of the production layer and depth of concentration peak for every aquatic microorganism species, while the sinking velocity is strictly connected with the phytoplankton size. Moreover, it is known that growth rates and nutrient uptake play a main role in the balance of a marine ecosystem [6,46,47], and contribute to modify the composition of the phytoplankton communities.

In this paper we investigate two sites of the Strait of Sicily, localized between the eastern and western basins of Mediterranean Sea and characterized by weakly mixed water. The purpose of this work is to simulate the spatio-temporal distributions of two groups of picophytoplankton, i.e. picoeukaryotes and *Prochlorococcus*, which account about for 60% of total *chl a* and *Dvchl a* concentration on average in Mediterranean Sea [48,49]. In order to study our marine ecosystem, it is necessary to set the correct values of the parameters. These have to guarantee the coexistence of the two groups [4,50], i.e. picoeukaryotes and *Prochlorococcus*, in the deep chlorophyll maximum (DCM).

Initially we use a deterministic advection-reaction-diffusion model to analyze the spatio-temporal evolution of the biomass concentrations of both groups, obtaining the distributions of the total *chlorophyll a* (*chl a*) and *divinil chlorophyll a* (*Dvchl a*) concentrations in stationary regime. Afterwards, in order to take into account the randomly fluctuating behaviour of the environmental variables, we study the ecosystem dynamics by a stochastic approach, by inserting terms of multiplicative Gaussian noise in the system equations. The numerical results are compared with experimental data sampled in two different sites of the Sicily Channel.

## Environmental Data

Data used in this work were acquired in the period 12<sup>th</sup>–24<sup>th</sup> August 2006 in the Sicily Channel area (Fig. 1) during the MedSudMed-06 Oceanographic Survey onboard the R/V *Urania*. Conductivity, temperature and density were sampled by means of the SBE911 plus CTD probe (Sea-Bird Inc.), while *chlorophyll a* and *divinil chlorophyll a* fluorescence measurements (*chl a/divinil chl a*,  $\mu\text{g l}^{-1}$ ) were contemporary performed using the Chelsea Aqua 3 sensor. The CTD stations were located on a grid of 12×12 nautical miles in Mediterranean Sea, and the values of oceanographic parameters were collected along a transect between

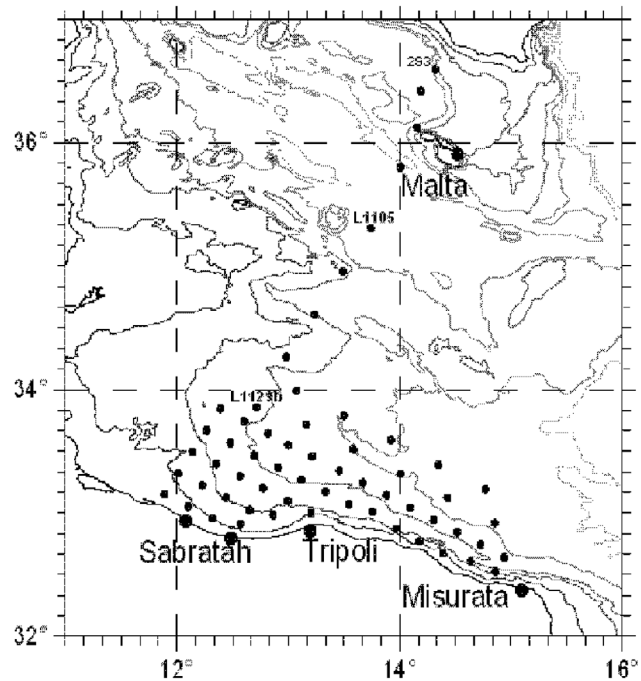


**Figure 1. Locations of the CTD stations where the experimental data were collected. (Courtesy of Valenti et al., 2012 (Ref. [27])).**

doi:10.1371/journal.pone.0066765.g001

the Sicilian and the Libyan coasts. The collected data were processed, generating a text file for each station, where the values of the experimental data were estimated with a 1 m step.

In this work, two sites out of the whole data set were considered. In particular, the selected stations were located at south of Malta (site L1105) and on the Libyan continental shelf (site L1129b) (see Fig. 1). Here, hydrological parameters remained constant for the entire sampling period and were representative of the oligotrophic Mediterranean Sea in summer [34]. Nutrient concentrations, i.e. nitrate and phosphate, were not sampled.

## Phytoplanktonic Data

The quantity that indicates the presence of phytoplankton biomass in marine environment is the concentration of *chlorophyll a* and *divinil chlorophyll a* [48,51]. Moreover, the contribution of each phytoplankton group to the total phytoplankton biomass is obtained using group-specific conversion factors empirically determined, and based on the analysis of taxonomic pigments [52,53]. These pigments have been used as size class markers of two main size fractions: picophytoplankton ( $<3\mu\text{m}$ ) and nano- and micro-phytoplankton ( $>3\mu\text{m}$ ).

The picophytoplankton size fraction accounts for 80% of the total *chl a* and *Dvchl a* on average in the Strait of Sicily, and is mainly represented by two groups: picoprokaryotes and picoeukaryotes. The picoprokaryotes group is dominated by two species of cyanobacteria, i.e. *Synechococcus* and *Prochlorococcus*, while picoeukaryotes group is mainly represented by pelagophytes and prymnesiophytes [48]. *Prochlorococcus*, *Synechococcus* and picoeukaryotes are usually identified and measured based upon their scattering and autofluorescence [48]. This is due to the presence of *chl a* or *Dvchl a* molecules in their cells. Finally, *Prochlorococcus* and picoeukaryotes contribute equally to the picophytoplankton in terms of *chl a* and *Dvchl a* concentrations,

even if *Prochlorococcus* are numerically more abundant than the picoeukaryotes group [51].

The nano- and micro-phytoplankton fraction amounts in average to 20% of the total *chl a* and *Dvchl a* and is uniformly distributed along the water column. This size fraction is dominated by prymnesiophytes and diatoms.

Picophytoplankton groups present eco-physiological properties [54–57] that make them appropriate to be studied by the use of biological models. In fact, the small size of *Prochlorococcus* and picoeukaryotes leads to a low package effect, which contributes to the light-saturated rate of photosynthesis that can be achieved at relatively low irradiances [54,58–60]. This feature allows the growth of picoeukaryotes in deeper layers of the water column. Conversely, a low nutrient uptake of picoeukaryotes leads to an enough high nutrient concentration in shallower layers of the water column, where *Prochlorococcus* are localized and their growth is allowed. Because of their peculiarities and relevant role in the functioning of the ecosystem, *Prochlorococcus* and picoeukaryotes constitute two populations that can coexist in same marine environment. In these conditions they are suitable to be described by a model of population dynamics [3,4,50].

In the Strait of Sicily [48,51,53], the average picoeukaryotes concentration in the DCM is  $0.6 \pm 0.4 \times 10^3$  cell ml<sup>-1</sup>, and the mean value of *chl a* cell<sup>-1</sup> ranges between 10 and 660 fg *chl a* cell<sup>-1</sup> along the water column, with a significant exponential increase with depth (see Fig. 2a) [5]. The concentration of *chl a* per cell in picoeukaryotes is highly variable among different water masses, with significantly higher values in the DCM respect to the surface [55,59,61,62].

In our ecosystem, picophytoplankton is numerically dominated by *Prochlorococcus* with average concentrations of  $5.2 \times 10^4$  cell ml<sup>-1</sup>. This species is more concentrated in DCM, where can achieve the mean value of  $12.5 \times 10^4$  cell ml<sup>-1</sup>. In particular, the marker of *Prochlorococcus* is *divinil chlorophyll a*, whose molecular structure is almost identical to that of *chlorophyll a*. The *Dvchl a* cellular content of total *Prochlorococcus* ranges between 0.25 and 2.20 fg *Dvchl a* cell<sup>-1</sup> along the water column, with a mean value exponentially increasing with depth (see Fig. 2b) [51].

Experimental analysis performed on samples collected in Sargasso Sea and Mediterranean Sea showed that the cellular content of *chl a* and *Dvchl a* increases in *Prochlorococcus* and *Synechococcus* with decreasing light intensity [63]. In particular, ranging from 1500  $\mu\text{mol photons m}^{-2} \text{s}^{-1}$  near the surface to less than 1  $\mu\text{mol photons m}^{-2} \text{s}^{-1}$  below the euphotic zone (approximately 100 m in Mediterranean Sea during the summer period), cells display a variety of differences. The most obvious ones are concomitant increases in cell size and pigment content, which generally occur below the depth of the mixed layers [64]. On the other side, for depth greater than 100 m, the cell concentration of picophytoplankton shows a considerable decrease, due to the dramatic diminution of the light intensity, which becomes less than 1% of the light intensity at the sea surface. The consequent strong reduction of cell concentration below euphotic zone allows to exploit the conversion curves shown in Fig. 2 also for depth below 100 m, describing, without significative errors, the increase in pigment content per cell.

In general, picophytoplankton ranges from 40% to 90% of total *chl a* along the water column, with an average value of 69% close to the DCM. Picoprotokaryotes are dominant in the first 50 meters, but are replaced by picoeukaryotes in deeper water [51].

The fluorescence profiles for *chl a* concentration, acquired in the Sicily Channel during the MedSudMed-06 Oceanographic Survey, show a nonmonotonic behaviour, as a function of the depth, characterized by the presence of DCM in both sites (see Fig. 3). In particular, the *chlorophyll a* concentrations range between 0.01 and 0.17  $\mu\text{g chl a l}^{-1}$ , with a deep chlorophyll maximum always present between 87 and 111 m depth. Finally, we observed different depth, shape and width of the DCM in the two sites studied.

## Methods

The spatio-temporal behaviour of the two picophytoplankton groups is analyzed by using a stochastic model with conditions typical of the Mediterranean Sea, where the vertical water columns are weakly mixed. In Fig. 4 we give a schematic representation of the mechanism underlying the phytoplankton dynamics. The mathematical tool used to simulate the picophy-

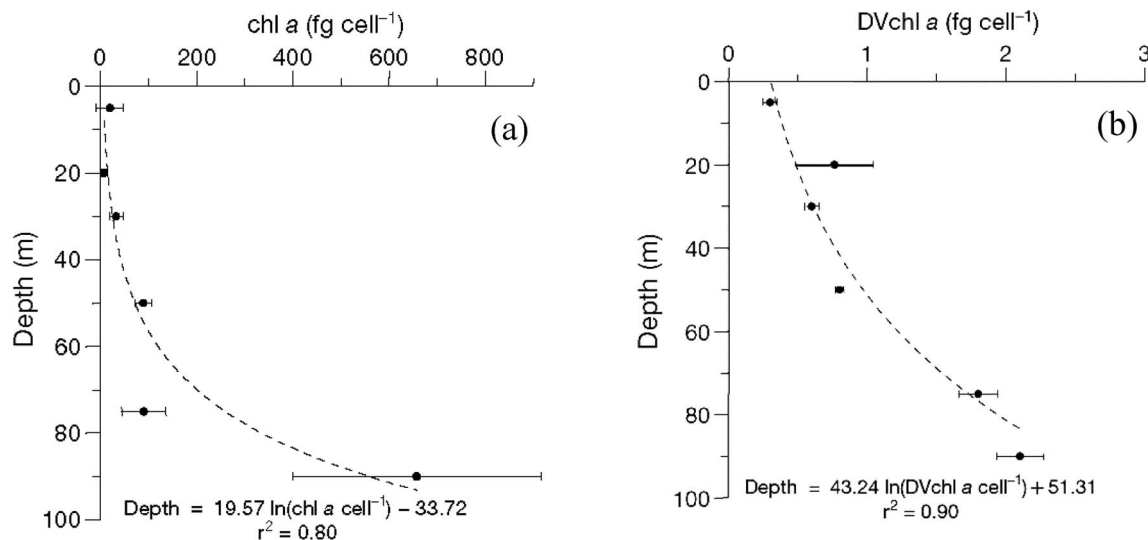


**Figure 2. Mean vertical profile of *chl a* per picoeukaryote cell (panel a) and *Dvchl a* per *Prochlorococcus* cell (panel b).** Error bars are Standard Deviation. Equation and  $r^2$  for the fit are reported on the plots. (Courtesy of Brunet et al., 2007 (Ref. [51])). doi:10.1371/journal.pone.0066765.g002

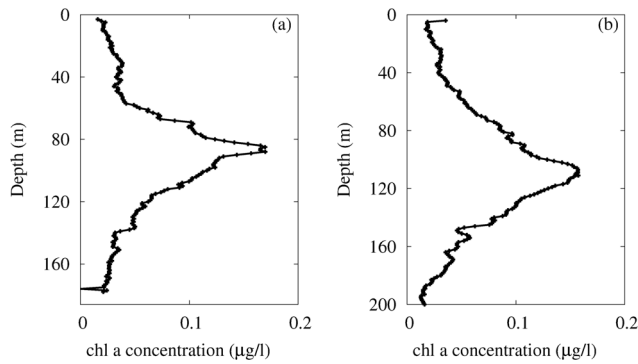


**Figure 3. Profiles of chl a concentration measured in sites L1129b (panel a) and L1105 (panel b).** The black lines have been obtained by connecting the experimental points corresponding to samples distanced of 1 meter along the water column. The total number of samples measured in the two sites is  $n=176$  for L1129b, and  $n=563$  for L1105. (Courtesy of Denaro et al., 2013 (Ref. [28])). doi:10.1371/journal.pone.0066765.g003

toplankton dynamics is an advection-reaction-diffusion model. The analysis is performed considering two different populations: (i) picoeukaryotes group; (ii) Prochlorococcus, which is a species belonging to the picoprokaryotes group. Analysis and numerical elaborations are divided in two phases:

- *Phase 1.* The distributions of biomass concentrations  $b_1(z,t)$  (picoeukariotes) and  $b_2(z,t)$  (Prochlorococcus), and nutrient concentration  $R(z,t)$  are obtained along the weakly mixed water column as a function of the time  $t$  and depth  $z$ , by using a deterministic model based on three differential equations. The results obtained are in a good qualitative agreement with the experimental data collected in the two different sites of the Strait of Sicily.
- *Phase 2.* In order to obtain, from a quantitative point of view, a more significative agreement between theoretical results and experimental data, the random fluctuations of the environmental variables are taken into account. In particular, a stochastic model is devised, starting from the deterministic one and inserting into the equations terms of multiplicative Gaussian noise. Specifically, as a first step, a term of multiplicative noise is added only in the differential equation for the nutrient concentration (case 1). As a second step, terms of multiplicative noise are inserted also into the equations for the biomass concentrations of picoeukariotes and Prochlorococcus (case 2). By this way, the effects of the environmental noise on picophytoplankton distributions are analyzed.

### The Deterministic Model

In this section, we consider a deterministic advection-reaction-diffusion model [2–4] to analyze the dynamics of the two picophytoplanktonic groups, distributed along a one-dimensional spatial domain ( $z$ -direction). In particular, we assume that the interaction of these populations with the environment occurs through two factors that limit the growth of the aquatic microorganisms: light intensity and nutrient, i.e. phosphorus. The model allows to obtain the dynamics of the biomass concentrations of picoeukaryotes and Prochlorococcus,  $b_1(z,t)$  and  $b_2(z,t)$ , nutrient concentration  $R(z,t)$  and light intensity  $I(z,t)$ . A crucial role in the phytoplankton dynamics is played by three different factors: growth and loss of biomass concentration, and movement of the single microorganisms.

The growth rates of the two picophytoplankton groups are strictly connected with  $I$  and  $R$ , whose characteristics of limiting factors [2,33,41,65] are implemented in the model by the Monod kinetics [66]. The gross phytoplankton growth rates per capita are given by  $\min\{f_i(I),f_{R_i}(R)\}$ , where  $f_i(I)$  and  $f_{R_i}(R)$  are obtained by the Michaelis-Menten formulas

$$f_i(I) = r_i I / (I + K_{I_i}), \quad (1)$$

$$f_{R_i}(R) = r_i R / (R + K_{R_i}). \quad (2)$$

where  $r_i$  is the maximum growth rate, and  $K_{I_i}$  and  $K_{R_i}$  are the half-saturation constants for light intensity and nutrient concentration, respectively, of the  $i$ -th picophytoplankton group. These constants depend on the metabolism of the specific microorganisms considered. In particular,  $K_{R_i}$  and  $K_{I_i}$  contribute to determine the position along the water column (depth) of the maximum (peak) of biomass concentration for each species. The biomass loss of the  $i$ -th picophytoplankton group, connected with respiration, death, and grazing, occurs at a rate  $m_i$  [2–4]. The gross per capita growth rates are defined as

$$g_i(z,t) = \min(f_{R_i}(R(z,t)), f_i(I(z,t))). \quad (3)$$

The movement of phytoplankton groups depends on turbulence, responsible for a passive movement of the phytoplankton. Turbulence is modeled by vertical diffusion coefficient  $D$ , which we assume uniform with the depth in both sites. Sinking velocities of the two picophytoplankton groups,  $v_1$  and  $v_2$ , describe another passive movement of picoeukaryotes and picoprokaryotes along water column towards deeper layers [2,50,67]. Positive velocities are oriented downward (sinking) for both groups, and are set equal to those observed in experimental data [3,4].

Taken together, these assumptions about growth, loss, and movement result in the following differential equations for the dynamics of the biomass concentrations of picoeukaryotes  $b_1(z,t)$  and Prochlorococcus  $b_2(z,t)$  [3,4,50].

$$\begin{aligned} \frac{\partial b_1(z,t)}{\partial t} &= b_1 \min(f_{I_1}(I), f_{R_1}(R)) - m_1 b_1 \\ &+ D \frac{\partial^2 b_1(z,t)}{\partial z^2} - v_1 \frac{\partial b_1(z,t)}{\partial z} \end{aligned} \quad (4)$$

$$\begin{aligned} \frac{\partial b_2(z,t)}{\partial t} &= b_2 \min(f_{I_2}(I), f_{R_2}(R)) - m_2 b_2 \\ &+ D \frac{\partial^2 b_2(z,t)}{\partial z^2} - v_2 \frac{\partial b_2(z,t)}{\partial z}. \end{aligned} \quad (5)$$

Boundary conditions for concentrations of picoeukaryotes and Prochlorococcus biomass describe no-flux in both surface layer  $z=0$  and seabed  $z=z_b$ :

$$\left[ D \frac{\partial b_i}{\partial z} - v_i b_i \right]_{z=0} = \left[ D \frac{\partial b_i}{\partial z} - v_i b_i \right]_{z=z_b} = 0. \quad (6)$$

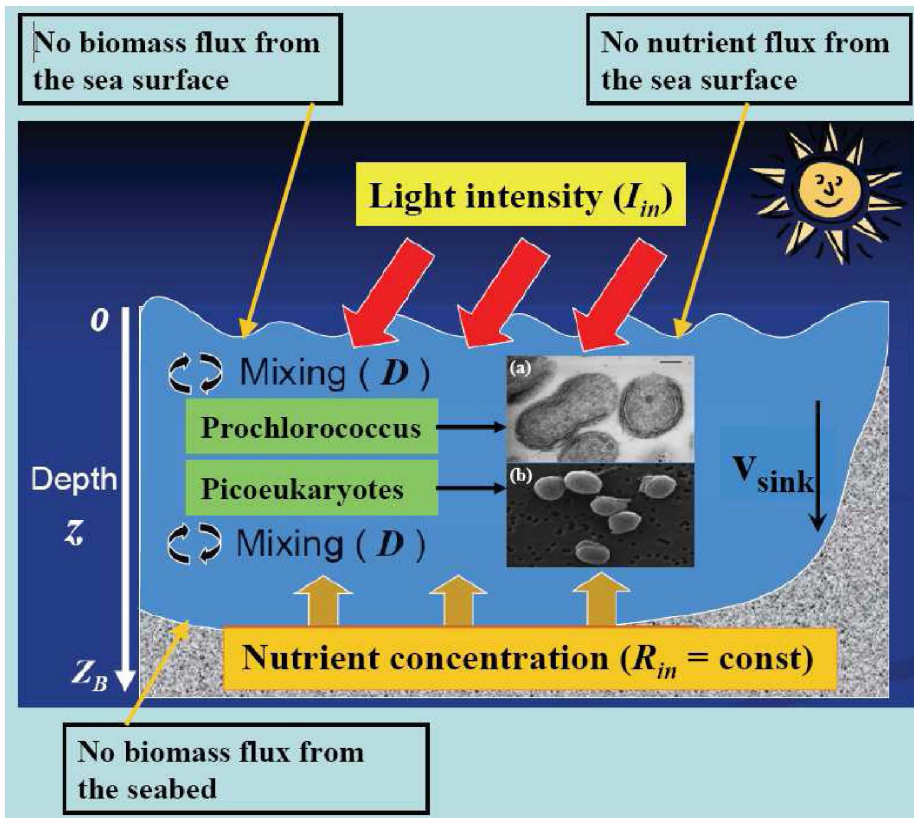


**Figure 4. Scheme of the mechanism responsible for the phytoplankton dynamics (modified from original figure by Alexey Ryabov).** Inset: (a) *Prochlorococcus* PCC 9511 (courtesy of Rippka et al., 2000 (Ref. [99])), (b) *Micromonas* NOUM17 (courtesy of Augustin Engman, Rory Welsh, and Alexandra Worden). (Color online). doi:10.1371/journal.pone.0066765.g004

The nutrient concentration  $R(z,t)$  is consumed by both the picophytoplankton groups, and a further quantity of nutrient is obtained from dead phytoplankton by a recycling process. Furthermore, turbulence is also responsible for mixing of the nutrient concentration along the water column and it is described by the vertical diffusion coefficient  $D$ . All these processes are modeled by the following equation.

$$\frac{\partial R(z,t)}{\partial t} = - \sum \frac{b_i(z,t)}{Y_i} \cdot \min(f_{I_i}(I), f_{R_i}(R)) + D \frac{\partial^2 R(z,t)}{\partial z^2} + \sum \varepsilon_i m_i \frac{b_i(z,t)}{Y_i} \quad (7)$$

where  $\varepsilon_i$  and  $1/Y_i$  are nutrient recycling coefficient and nutrient content of the  $i$ -th picophytoplankton group, respectively.

Nutrients do not come from the top of the water column but are supplied from the bottom. In particular, nutrient concentration at the bottom of the water column,  $R(z_b)$ , is fixed at value  $R_{in}$ , which is different in the two sites investigated. Thus the boundary conditions are described by the following equations:

$$\frac{\partial R}{\partial z} \Big|_{z=0} = 0, \quad R(z_b) = R_{in}. \quad (8)$$

The light intensity is assumed to decrease exponentially according to Lambert-Beer's law [5,68,69].

$$I(z) = I_{in} \exp \left\{ - \int_0^z \left[ \sum a_i b_i(Z) + a_{bg} \right] dZ \right\} \quad (9)$$

where  $a_i$  are the absorption coefficients of the  $i$ -th picophytoplankton group,  $a_{bg}$  is the background turbidity, and  $I_{in}$  is the incident light intensity at the water surface.

### The Stochastic Model

The theoretical model discussed in the previous section is based on a deterministic approach. However, it is worth to recall that the marine ecosystems are complex systems, that is open systems characterized by non-linear interactions [14,25,28,70–77]. In particular, each picophytoplankton group not only interacts with all other populations, but is also subject to environmental variables, such as turbulence and availability of food resources, which affects the ecosystem dynamics through deterministic and random perturbations. In this context, random variations of species concentrations [7–9,18,21] are fundamental aspects that can not be neglected when seeking a better understanding of the dynamics of complex living systems. Here the fluctuations of temperature, food resources, and other environmental parameters can be modeled by including multiplicative noise sources [10,11,14,70], that can effectively reproduce experimental data in population dynamics [78–80].

We note that the same arguments hold for nutrients, whose random fluctuations should be modeled by terms of multiplicative noise, according to the approach widely used to describe stochastic dynamics not only in physics, but also in biology, ecology, economy, or social sciences [79]. This agrees with the observation that the effects of fluctuations have to be proportional to the activity densities [81–85], which are in our system the biomass and nutrient concentrations.

We recall also that problems, which involve absorbing states, are described by equations whose noise amplitude is proportional to the square root of the space and time dependent activity density. Such systems include propagating epidemics, autocatalytic reactions, and reaction-diffusion problems [79].

Finally we underline that in our ecosystem biomass and nutrient concentrations are affected by unpredictable changes mainly generated by two sources of fluctuations: i) vertical mixing along the water column due to the random variations of the velocity field, ii) gain or loss of biomass and nutrient concentrations among different water columns due to random horizontal movement. Thus the multiplicative noise, used in population dynamics and reaction-diffusion problems [78,86–88], within our specific physical and biological context describes the two above mentioned noise sources. These are responsible for the real behaviour of the ecosystem, characterized by an intrinsically non-deterministic dynamics.

Therefore, in order to reproduce the dynamics of the picophytoplankton groups and nutrient concentration, taking into account the role of environmental fluctuations, we modify the model given by Eqs. (4)–(9), including terms of multiplicative noise.

**Case 1.** The environmental noise affects only the nutrient concentration. In this case, Eqs. (4),(5),(6),(8),(9) remain unchanged, while Eq. (7) is replaced by

$$\begin{aligned} \frac{\partial R(z,t)}{\partial t} = & - \sum \frac{b_i(z,t)}{Y_i} \cdot \min(f_{I_i}(I), f_{R_i}(R)) + D \frac{\partial^2 R(z,t)}{\partial z^2} \\ & + \sum \varepsilon_i m_i \frac{b_i(z,t)}{Y_i} + R \xi_R(z,t). \end{aligned} \quad (10)$$

**Case 2.** The environmental noise affects the concentrations of picoeukaryotes biomass, Prochlorococcus biomass and nutrient. Therefore, Eqs. (6),(8),(9) are the same, while Eqs. (4),(5) and (7) become.

$$\begin{aligned} \frac{\partial b_1(z,t)}{\partial t} = & b_1 \min(f_{I_1}(I), f_{R_1}(R)) - m_1 b_1 + D \frac{\partial^2 b_1(z,t)}{\partial z^2} - v_1 \frac{\partial b_1(z,t)}{\partial z} \\ & + b_1 \xi_{b_1}(z,t) \end{aligned} \quad (11)$$

$$\begin{aligned} \frac{\partial b_2(z,t)}{\partial t} = & b_2 \min(f_{I_2}(I), f_{R_2}(R)) - m_2 b_2 + D \frac{\partial^2 b_2(z,t)}{\partial z^2} - v_2 \frac{\partial b_2(z,t)}{\partial z} \\ & + b_2 \xi_{b_2}(z,t) \end{aligned} \quad (12)$$

$$\begin{aligned} \frac{\partial R(z,t)}{\partial t} = & - \sum \frac{b_i(z,t)}{Y_i} \cdot \min(f_{I_i}(I), f_{R_i}(R)) + D \frac{\partial^2 R(z,t)}{\partial z^2} \\ & + \sum \varepsilon_i m_i \frac{b_i(z,t)}{Y_i} + R \xi_R(z,t). \end{aligned} \quad (13)$$

Here  $\xi_{b_1}(z,t)$ ,  $\xi_{b_2}(z,t)$  and  $\xi_R(z,t)$  are statically independent and spatially uncorrelated white Gaussian noises with the following properties:  $\langle \xi_{b_i}(z,t) \rangle = 0$ ,  $\langle \xi_R(z,t) \rangle = 0$ ,  $\langle \xi_{b_i}(z,t) \xi_{b_j}(z',t') \rangle = \sigma_{b_i} \delta(z-z') \delta(t-t')$ ,  $\langle \xi_R(z,t) \xi_R(z',t') \rangle = \sigma_R \delta(z-z') \delta(t-t')$ , with  $i=1,2$ . Here  $\sigma_{b_i}$  and  $\sigma_R$  are the intensities of the noise sources which act on the  $i$ -th picophytoplanktonic group and nutrient, respectively.

### Simulation Setting

In order to reproduce the spatial distributions observed in the experimental data for the total concentration of *chl a* and *Dvchl a* (see Fig. 3), we choose the values of the environmental and biological parameters so that the monostability condition is obtained. This corresponds to the presence of a deep chlorophyll maximum for both picophytoplankton groups [2–4,28], which coexist in the same ecosystem even if the maximum concentration for each group is localized at a different depth [5]. The numerical values assigned to the parameters are shown in Table 1.

The values of the biological parameters have been chosen to reproduce the behaviour of picoeukaryotes and Prochlorococcus. In particular, for both groups, the maximum specific growth rates are in agreement with ones measured from other authors [89] and the sinking velocity is set to the typical value for picophytoplankton,  $v=0.1 \text{ m day}^{-1}$  [3]. The half-saturation constants,  $K_{R_i}$  and  $K_{I_i}$ , for the two groups are set to obtain a suitable position of production layers and a certain depth for the position of the peak of biomass concentration. Since picoeukaryotes consist of picophytoplankton species that are better adapted to lower light intensity than Prochlorococcus, we fix  $K_{I_1} < K_{I_2}$ . Viceversa, since Prochlorococcus is better adapted to lower nutrient concentration than picoeukaryotes group, we set  $K_{R_2} < K_{R_1}$ . As a consequence, the peak of picoeukaryotes concentration along the water column tends to be deeper than the peak of Prochlorococcus concentration. It is worth noting that the nutrient content of the picoeukaryotes,  $1/Y_1$ , is set to different values in the two sites investigated in this work. This choice can be explained recalling that, in the Mediterranean Sea, the picoeukaryotes group located in DCM includes several species. As a consequence, depending of the marine site analyzed, different ecotypes of this group prevail and nutrient content changes accordingly [6,90]. Viceversa, the nutrient content of picoprokaryotes ( $1/Y_2$ ) is set equal in both sites because Prochlorococcus is the only species of its group present in DCM. We recall that the parameters  $1/Y_1$  and  $1/Y_2$  contribute to determine the steady distributions of the picophytoplankton concentrations. Experimental findings indicate that (i) the peak of biomass concentration of Prochlorococcus is shallower than that of picoeukaryotes and (ii) the cell concentration of Prochlorococcus is much higher than that of picoeukaryotes. In these conditions a smaller amount of nutrient is available for Prochlorococcus localized in the biomass peak. Therefore, in order to obtain for the two picophytoplankton groups, the correct cell concentrations as found in field observations,  $1/Y_2$  is set at a value much smaller than  $1/Y_1$  (see Table 1). The absorption coefficient of Prochlorococcus, fixed in our model, is very different from that of the



**Table 1.** Parameters used in the model.

Symbol	Quantity	Unit	Site L1129b	Site L1105
$I_{in}$	Incident light intensity	$\mu\text{ mol photons m}^{-2}\text{ s}^{-1}$	1404.44	1383.19
$a_{bg}$	Background turbidity	$\text{m}^{-1}$	0.045	0.045
$a_1$	Absorption coefficient of picoeukaryotes	$\text{m}^2\text{ cell}^{-1}$	$6 \times 10^{-10}$	$3.3 \times 10^{-10}$
$a_2$	Absorption coefficient of Prochlorococcus	$\text{m}^2\text{ cell}^{-1}$	$2.4 \times 10^{-15}$	$2.4 \times 10^{-15}$
$z_b$	Depth of the water column	m	186	575
$D$	Vertical turbulent diffusivity	$\text{cm}^2\text{ s}^{-1}$	1.0	3.0
$r_1$	Maximum specific growth rate of picoeukaryotes	$\text{h}^{-1}$	0.08	0.08
$r_2$	Maximum specific growth rate of Prochlorococcus	$\text{h}^{-1}$	0.07	0.07
$K_{I_1}$	Half-saturation constant of light-limited growth of picoeukaryotes	$\mu\text{ mol photons m}^{-2}\text{ s}^{-1}$	20	20
$K_{R_1}$	Half-saturation constant of nutrient-limited growth of picoeukaryotes	$\text{mmol nutrient m}^{-3}$	0.0425	0.0425
$K_{I_2}$	Half-saturation constant of light-limited growth of Prochlorococcus	$\mu\text{ mol photons m}^{-2}\text{ s}^{-1}$	98	98
$K_{R_2}$	Half-saturation constant of nutrient-limited growth of Prochlorococcus	$\text{mmol nutrient m}^{-3}$	0.0150	0.0150
$m_1$	Specific loss rate of picoeukaryotes	$\text{h}^{-1}$	0.01	0.01
$m_2$	Specific loss rate of Prochlorococcus	$\text{h}^{-1}$	0.01	0.01
$1/Y_1$	Nutrient content of picoeukaryotes	$\text{mmol nutrient cell}^{-1}$	$1 \times 10^{-9}$	$0.6 \times 10^{-9}$
$1/Y_2$	Nutrient content of Prochlorococcus	$\text{mmol nutrient cell}^{-1}$	$4 \times 10^{-15}$	$4 \times 10^{-15}$
$\varepsilon_1$	Nutrient recycling coefficient of picoeukaryotes	dimensionless	0.5	0.5
$\varepsilon_2$	Nutrient recycling coefficient of Prochlorococcus	dimensionless	0.5	0.5
$v_1$	Sinking velocity of picoeukaryotes	$\text{m h}^{-1}$	0.0042	0.0042
$v_2$	Sinking velocity of Prochlorococcus	$\text{m h}^{-1}$	0.0042	0.0042
$R_{in}$	$z_b$ Nutrient concentration at	$\text{mmol nutrient m}^{-3}$	5.0	6.0

The values of the biological parameters are those typical of picoeukaryotes and Prochlorococcus.  
doi:10.1371/journal.pone.0066765.t001

picoeukaryotes. In fact, due to the low nutrient concentration in higher layers and different average cell concentration of the two groups ( $0.6 \times 10^3$  cells  $\text{ml}^{-1}$  for picoeukaryotes and  $5.2 \times 10^4$  cells  $\text{ml}^{-1}$  for Prochlorococcus), we had to exploit an absorption coefficient for Prochlorococcus lower than that used for picoeukaryotes. In particular, in order to obtain the same gradient of light intensity inside the production layers [50], we set  $a_2 = 2.4 \times 10^{-15} \text{m}^2 \text{cell}^{-1}$ . All the other biological parameters are the same in both sites in agreement with ones used from other authors [3,4].

The values of the environmental parameters have been chosen to reproduce marine ecosystem of Sicily Channel in summer, i.e. oligotrophic water and high light intensity. The water column depths used in the model are fixed according to those measured in the corresponding marine sites. The diffusion coefficients are fixed at typical values of weakly mixed water ( $D = 1.0 \text{cm}^2 \text{s}^{-1}$  for site L1129b and  $D = 3.0 \text{cm}^2 \text{s}^{-1}$  for site L1105). This choice is due to the fact that the site L1129b is placed on the Libyan continental shelf, not far from the coast, where turbulence is low. Conversely, the site L1105 is located in the middle of Sicily Channel, where vertical diffusion coefficient is greater respect to the Libyan coast because the flow of the Modified Atlantic Water (MAW) and

Levantine Intermediate Water (LIW) are responsible for a bigger turbulence. Moreover, we set that the light intensity at the water surface,  $I_{in}$ , is larger than  $1300 \mu\text{mol photons m}^{-2} \text{s}^{-1}$  in both sites. This is due to the fact that the sampling of the experimental data occurred during summer (August 2006), when the light intensity achieves maximum values in Mediterranean Sea. In particular, the light intensities used in this study were fixed using data available on the NASA web site (<http://eosweb.larc.nasa.gov/sse/RETSscreen/>). Finally, nutrient concentrations at depth  $z_b$  were fixed at values such as to obtain, for each site, a peak of biomass concentration at the same position of the peak experimentally observed.

## Results

The spatio-temporal dynamics of the biomass and nutrient concentrations are obtained by numerically integrating Eqs. (4)–(9). The numerical method, whose computer implementation consists in a C++ program, exploits an explicit finite difference scheme. In order to get the steady spatial distributions, we solved numerically our equations over a time interval long enough to achieve the stationary solution [91]. As initial conditions, for each

marine sites analyzed, we fixed that the picoeukaryotes and Prochlorococcus biomasses are concentrated in two layers close to the deep chlorophyll maximum experimentally observed. On the other side, the phosphorus concentration decrease linearly above seabed up to DCM, while remain approximately constant from this point to the water surface.

### Solution by Deterministic Approach

A preliminary analysis (results here not shown) indicates that large values of  $I_m$  lead to stationary conditions characterized by the presence of a DCM, where two species can coexist, while large values of  $R_m$  (nutrient concentration close to seabed) determine an upper chlorophyll maximum (UCM) [4], where picoeukaryotes prevail and Prochlorococcus undergoes a strong reduction. In particular, for fixed values of  $I_m$  and  $D$ , an increase of  $R_m$  generates a displacement of picoeukaryotes towards higher layers, where the production layer of Prochlorococcus is located. As a consequence of light limitation, Prochlorococcus moves upward in the direction of surface layers of the water column. If  $R_m$  is very high, we can observe an upper chlorophyll maximum (UCM) due to the picoeukaryotes group and the disappearance of Prochlorococcus. These results are in agreement with those shown in Ref. [50].

By solving Eqs. (4)–(9) for the maximum simulation time  $t_{max} = 5 \cdot 10^4 h$ , the stationary solution already appears for  $t \approx 3 \cdot 10^4 h$ . Therefore, in order to obtain the stationary distributions for the biomass concentrations of picoeukaryotes and Prochlorococcus, and the profile of light intensity, it is sufficient to set  $t_{max} = 4 \cdot 10^4 h$ . The results are shown in Fig. 5. We observe the presence of a picoeukaryotes biomass peak (panels a, d of Fig. 5) in correspondence of the two experimental DCMs (see Fig. 3). Moreover, a Prochlorococcus biomass peak (panels b, e of Fig. 5) is observed close to the two experimental DCMs (see again Fig. 3). Finally the typical exponential behaviour of the light intensity is found (panels c, f of Fig. 5).

We recall that our experimental data are expressed in  $\mu g/l$  (see Fig. 3), which is the unit of measure used for *chl a* and *Dvchl a* concentrations. Therefore, in order to compare the numerical results with experimental profiles, the theoretical cell concentrations of picoeukaryotes and Prochlorococcus (expressed in  $cell/m^3$ ) have been converted into *chl a* and *Dvchl a* concentrations (expressed in  $\mu g/l$ ) by using, respectively, the curves of mean vertical profile obtained by Brunet et al. [48,51]. Since the structure of the *chlorophyll a* molecule is almost identical to that of *Dvchlorophyll a*, we summed their concentrations to get theoretical equilibrium profiles consistent with those obtained from the experimental data. It is also important to recall that in Sicily Channel nano-phytoplankton, micro-phytoplankton and Synechococcus account about for 43% of the total quantity of *chl a* and *Dvchl a* [48,51]. This quantity is quite uniformly distributed along the water column. Therefore, we considered this fraction of the total biomass and divided it by depth, obtaining for each site the value  $\Delta b_{(Dv)chla}$ , which represents a constant concentration along the whole water column, due to other phytoplankton species present in the marine ecosystem [28]. Then, along the water column, we added the numerical concentrations with  $\Delta b_{(Dv)chla}$  and obtained, for both sites, the stationary theoretical profiles consistent with the experimental ones (see Fig. 6). Here it is possible to observe a fairly good agreement between experimental data (green line) and numerical results (red line). However, in site L1129b the theoretical distribution of *chl a* and *Dvchl a* is characterized by a shape quite different from that of the experimental profile. Moreover, in site L1105 we note that the

magnitude of the theoretical DCM is larger than that obtained from the real data. Finally, we performed a quantitative comparison based on the goodness-of-fit test  $\chi^2$ . The results (here not shown) indicate that, respect to the one-species model, this description provides in both sites theoretical results in a better agreement with the experimental findings [27,28].

### Solution by Stochastic Approach

In this section we perform the analysis of the stochastic model by numerically solving the corresponding equations. About the numerical integration, we recall that the calculus of stochastic differential equations with terms of white noise can be based on different definitions, i.e. Ito and Stratonovich schemes. This situation has led to a long controversy in physical literature. In particular, the Stratonovich's choice is the only definition of stochastic integral leading to a calculus with classic rules within the context of functional analysis. Moreover, a principle of invariance of the equation under "coordinate transformation" is invoked to pick the Stratonovich integral as the "right" one and reject the Ito integral as the "wrong" one. The principle refers to an invariance of the form of the stochastic differential equation under a non-linear transformation of the system. This invariance does not possess any physical virtue, but it is only a different way to say that the Stratonovich calculus obeys the familiar classic rules. The only quantities that have to be invariant under a coordinate transformation are the probabilities. This condition is of course guaranteed in both calculi. Finally we note that in biological applications often environmental fluctuations have a correlation time that is much shorter than the generation span. This allows to model the external fluctuations as a white noise (see Ref. [92], pp. 101, 102). In our ecosystem the environmental fluctuations occur over time scales, ranging from some seconds to few minutes, which are much shorter than the generation time of biomass and nutrient [93]. This indicates that the condition of "rapidly fluctuating variables" is ensured, and as a consequence environmental random variations can be modelled by white noise sources.

On this basis we conclude that the specific problem can be treated by performing the integration of the stochastic differential equations within the Ito scheme.

In particular we obtain, for different values of the noise intensities, the concentration profiles averaged over 1000 realizations [14,94]. The presence of noise sources does not determine significant variations in the time necessary to reach the steady state. Therefore, accordingly to the deterministic analysis, in order to get the stationary solution, we solve the equations of the stochastic model fixing as a maximum time  $t_{max} = 4 \cdot 10^4 h$ .

**Case 1.** We get the average theoretical distributions of total *chl a* and *Dvchl a* concentration in each site (see Figs. 7 and 8), by following the same procedure as in deterministic approach.

Here, the results show that a decrease and a deeper localization of the DCMs, respect to the deterministic case, are present also for low noise intensities ( $\sigma_R$  between 0.001 and 0.010). In order to evaluate the agreement of each theoretical distribution (red line) with the corresponding experimental one (green line), we use two comparative methods:  $\chi^2$  goodness-of-fit test and Kolmogorov-Smirnov (K-S) test. The results are shown in Tables 2 and 3, where  $\tilde{\chi}^2$  indicates the reduced chi-square, while  $D(K-S)$  and  $P(K-S)$  are the maximum difference between the cumulative distributions and the corresponding probability for the K-S test, respectively. The black lines have been obtained by connecting the experimental points corresponding to samples distanced of 1 meter along the water column. The quantitative comparison, based on the  $\chi^2$  goodness-of-fit test, shows a good agreement between



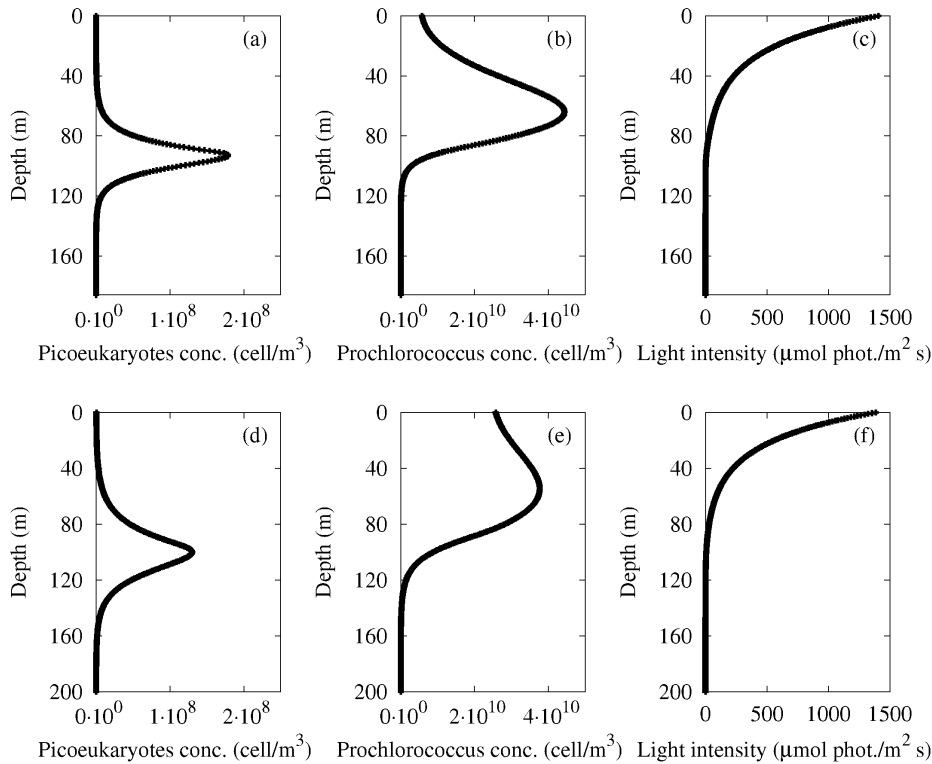


**Figure 5. Stationary distributions of picoeukaryotes and Prochlorococcus biomass concentrations and light intensity: site L1129b (panels a, b, c) and site L1105 (panels d, e, f) as a function of depth.**  
doi:10.1371/journal.pone.0066765.g005

theoretical and experimental profiles for both sites, better than in the deterministic case. In particular, the best value of the  $\chi^2$  test is obtained for site L1129b with  $\sigma_R = 0.0025$ , and for site L1105 with two different values of the noise intensity, i.e.  $\sigma_R = 0.0020$  and  $\sigma_R = 0.0025$ . Analyzing the results of the Kolmogorov-Smirnov test we get, in site L1105, the best agreement between experimental and theoretical distributions with  $\sigma_R = 0.0020$ , while in site L1129b the parameters  $D(K-S)$  and  $P(K-S)$  remain unchanged as  $\sigma_R$  varies. We note that the best agreement in site L1105 is obtained for a value of the noise intensity  $\sigma_R$  lower than that used in site L1129b. This can be explained by the fact that in

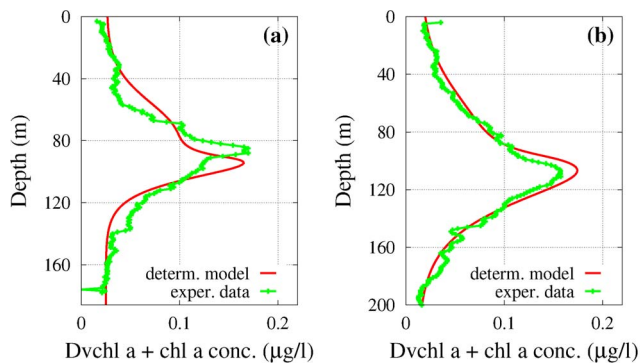


**Figure 6. Theoretical distributions (red line) of the total *chl a* and *Dvchl a* concentration in stationary conditions.** The profiles, obtained by the deterministic model and given as a function of the depth, are compared with experimental distributions (green line) sampled in sites L1129b (panel a) and L1105 (panel b). (Color online).  
doi:10.1371/journal.pone.0066765.g006

site L1105 the DCM is deeper than in site L1129b (111 m vs. 88 m). As a consequence, in site L1105 the environmental variables, and therefore the peak of total *chl a* and *Dvchl a* concentration, are subject to less intense random perturbations respect to site L1129b, which is closer to the water surface.

In order to better understand the dependence of the biomass concentration on the random fluctuations of the nutrient, we study for both sites the behaviour of the depth, width, and magnitude of the DCM as a function of  $\sigma_R$ . The results, shown in Fig. 9, indicate that the depth of the DCM slightly increases in both sites as a function of the noise intensity (see panels b, e). We note also that a decrease of the total concentration of *chl a* and *Dvchl a* is observed in the DCMs of the two sites (see panels a, d). At the same time we observe an increase, slightly faster in site L1105, of the width of the DCM (see panels c, f). The spread of DCM and reduction of its magnitude appear therefore to be strictly connected with each other. In general, the results (results here not shown) indicate that the phytoplankton biomass tends to disappear for  $\sigma_R > 0.01$ . On the basis of this analysis, the nutrient concentration appears to play a crucial role in the stability of both phytoplankton groups, i.e. picoeukaryotes and Prochlorococcus. The presence of noise sources directly acting on the nutrient concentration could explain, in real ecosystems, events as the disappearance of the picophytoplankton biomass.

**Case 2.** According to the procedure followed for case 1, we obtain in both sites the profiles of the total concentration of *chl a* and *Dvchl a* for suitable values of the noise intensity ( $\sigma_{b_1} = 0.22$ ,  $\sigma_{b_2} = 0.08$  and  $\sigma_R = 0.0025$  for site L1129b;  $\sigma_{b_1} = 0.15$ ,  $\sigma_{b_2} = 0.10$  and  $\sigma_R = 0.0020$  for site L1105). The results are shown in Fig. 10. In this case, the  $\chi^2$  goodness-of-fit test (see Table 4) exhibits values of the reduced chi-square ( $\tilde{\chi}^2 = 0.0019$  for site L1129b and

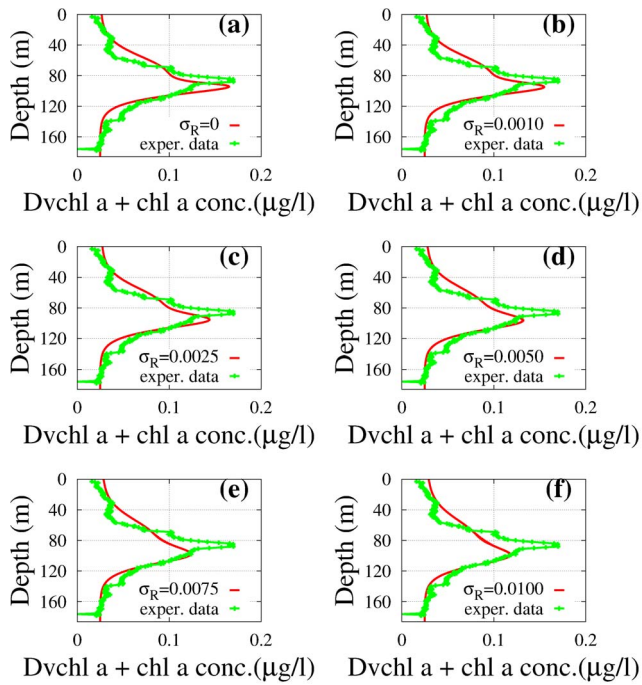


**Figure 7. Theoretical distributions (red line) of the total *chl a* and *Dvchl a* concentration (stochastic approach).** The profiles were obtained in stationary regime for different values of  $\sigma_R$  (case 1 of the stochastic model) as a function of depth. The results are compared with the distributions of the total *chl a* and *Dvchl a* concentration measured (green line) in site L1129b. The theoretical values were obtained averaging over 1000 numerical realizations. The values of the parameters are those shown in Table 1. The noise intensities are: (a)  $\sigma_R=0$  (deterministic case), (b)  $\sigma_R=0.0010$ , (c)  $\sigma_R=0.0025$ , (d)  $\sigma_R=0.0050$ , (e)  $\sigma_R=0.0075$  and (f)  $\sigma_R=0.0100$ . (Panels a and f: courtesy of Denaro et al., in press (Ref. [100])). (Color online). doi:10.1371/journal.pone.0066765.g007

$\chi^2 = 0.0008$  for site L1105) much lower than the values previously obtained from the stochastic approach in case 1. Viceversa, the statistical parameters,  $D(K-S)$  and  $P(K-S)$ , of the Kolmogorov-Smirnov test remain unchanged for site L1129b, while indicate in site L1105 a worse agreement, with respect to case 1, between numerical results and experimental data. On the basis of these results we can conclude that in site L1129b the presence of noise sources, which act on the phytoplankton biomass, allows to further improve the agreement between theoretical results and experimental findings. Contrasting indications are provided, in site L1105, by the  $\chi^2$  and K-S tests, about the role played by the noise sources  $\zeta_{b_1}$  and  $\zeta_{b_2}$  from the point of view of a better agreement between theoretical and experimental distributions.

In conclusion, the results obtained from the stochastic model indicate that the environmental fluctuations, connected with the random modifications of physical variables, such as temperature and salinity, can give rise to interesting effects: (i) “shift” of DCM towards a greater depth; (ii) “disappearance” of picoeukaryotes and *Prochlorococcus* for higher noise intensity. These results could explain the time evolution of picophytoplankton populations in real ecosystems whose dynamics is continuously influenced by random fluctuations of the environmental variables [7–9].

## Discussion

The work presented in this paper consisted in studying the dynamics of two picophytoplankton groups by using a stochastic

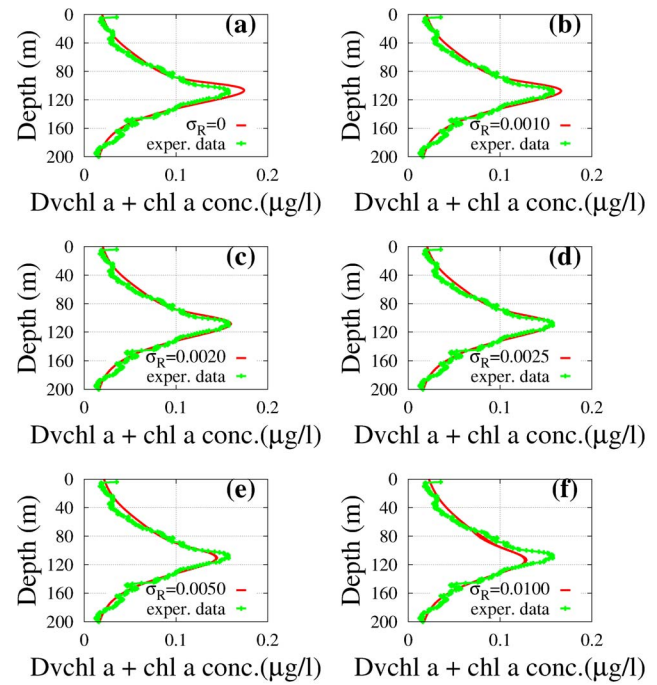


**Figure 8. Theoretical distributions (red line) of the total *chl a* and *Dvchl a* concentration (stochastic approach).** The profiles were obtained in stationary regime for different values of  $\sigma_R$  (case 1 of the stochastic model) as a function of depth. The results are compared with the distributions of the total *chl a* and *Dvchl a* concentration measured (green line) in site L1105. The theoretical values were obtained averaging over 1000 numerical realizations. The values of the parameters are those shown in Table 1. The noise intensities are: (a)  $\sigma_R=0$  (deterministic case), (b)  $\sigma_R=0.0010$ , (c)  $\sigma_R=0.0020$ , (d)  $\sigma_R=0.0025$ , (e)  $\sigma_R=0.0050$  and (f)  $\sigma_R=0.0100$ . (Color online). doi:10.1371/journal.pone.0066765.g008

model [27,28,70,73] and comparing the results with real data from the southern Mediterranean Sea. In particular we investigated two sites of the Strait of Sicily, where the waters are prevalently oligotrophic, i.e. with low nutrient concentrations, and the climatic parameters are those typical of a temperate region. The phytoplankton groups analyzed are picoeukaryotes and *Prochlorococcus*, which account about for 60% of total chlorophyll on

**Table 2. Results of  $\chi^2$ , reduced chi-square ( $\bar{\chi}^2$ ), and Kolmogorov-Smirnov goodness-of-fit tests for site L1129b with different values of  $\sigma_R$  (stochastic dynamics - case 1).**

$R_m$	$\sigma_R$	$\chi^2$	$\bar{\chi}^2$	D (K-S)	P (K-S)
5	0.0000	0.74	0.0042	0.1136	0.193
5	0.0010	0.69	0.0039	0.1136	0.193
5	0.0025	0.65	0.0037	0.1136	0.193
5	0.0050	0.66	0.0038	0.1136	0.193
5	0.0075	0.71	0.0041	0.1136	0.193
5	0.0100	0.78	0.0045	0.1136	0.193

D(K-S) and P(K-S) are the maximum difference between the cumulative distributions and the corresponding probability for the K-S test, respectively. The number of samples, used for the tests and distanced of 1 m, is  $n=176$ , corresponding to consider the whole water column. doi:10.1371/journal.pone.0066765.t002

**Table 3.** Results of  $\chi^2$ , reduced chi-square ( $\bar{\chi}^2$ ), and Kolmogorov-Smirnov goodness-of-fit tests for site L1105 at different values of  $\sigma_R$  (stochastic dynamics - case 1).

$R_m$	$\sigma_R$	$\chi^2$	$\bar{\chi}^2$	D (K-S)	P (K-S)
6	0.0000	0.23	0.0012	0.0812	0.517
6	0.0010	0.20	0.0010	0.0660	0.771
6	0.0020	0.18	0.0009	0.0609	0.847
6	0.0025	0.18	0.0009	0.0660	0.771
6	0.0050	0.19	0.0010	0.0711	0.687
6	0.0100	0.32	0.0016	0.1066	0.201

D(K-S) and P(K-S) are the maximum difference between the cumulative distributions and the corresponding probability for the K-S test, respectively. The number of samples, used for the tests and distanced of 1 m, is  $n = 200$ , corresponding to consider from the surface the first 200 m of depth. doi:10.1371/journal.pone.0066765.t003

average in Mediterranean Sea and belong to the smaller size fraction (less than  $3 \mu m$ ) of phytoplankton, i.e. picophytoplankton.

In general, the composition of phytoplankton changes along the water column between the surface and the seabed. This is due to the fact that different groups of picophytoplankton show different responses to the limiting factors, i.e. light intensity and nutrient concentration [6]. In particular, picoeukaryotes is a nutrient-limited group localized in deep chlorophyll maximum, viceversa Prochlorococcus is a light-limited species, which is forced to live close

to the light source. It is important to underline that, for larger values of depth, the light intensity becomes a main limiting factor for other species of picophytoplankton, such as Synechococcus, which show a low degree of adaptability to smaller values of light intensity [61,63] and, as a consequence, can not survive in deep layers of water column corresponding to DCM. For these reasons, we chose to analyze only the behaviour of Prochlorococcus and picoeukaryotes, which are characterized by a high degree of genetic plasticity [95] and a good adaptability to lower light intensities [55,63,96]. These two factors allow Prochlorococcus and picoeukaryotes to dominate in the deep chlorophyll maximum [51].

In this article, the competition between picoeukaryotes and Prochlorococcus for light and phosphorus sources has been modeled by using a advection-reaction-diffusion model [50,97]. Moreover, the values of the biological parameters, such as maximum specific growth rates and sinking velocities, are those of picoeukaryotes and Prochlorococcus, while some environmental parameters, such as incident light intensity and depth of the water column, are fixed at values obtained from real data. Finally, for the vertical turbulent diffusivity,  $D$ , and nutrient concentration at the bottom of the water column,  $R_m$ , we chose values suitable to reproduce, in stationary conditions, the deep chlorophyll maximum [4,50]. Both these parameters contribute to determine the nutrient availability along the water column and, as a consequence, to change the position, shape and magnitude of the peak of phytoplankton biomass [50]. Preliminary analysis showed that an increase of  $R_m$  favors the better light competitor, i.e. picoeukaryotes, viceversa an increase of  $D$  favors the better

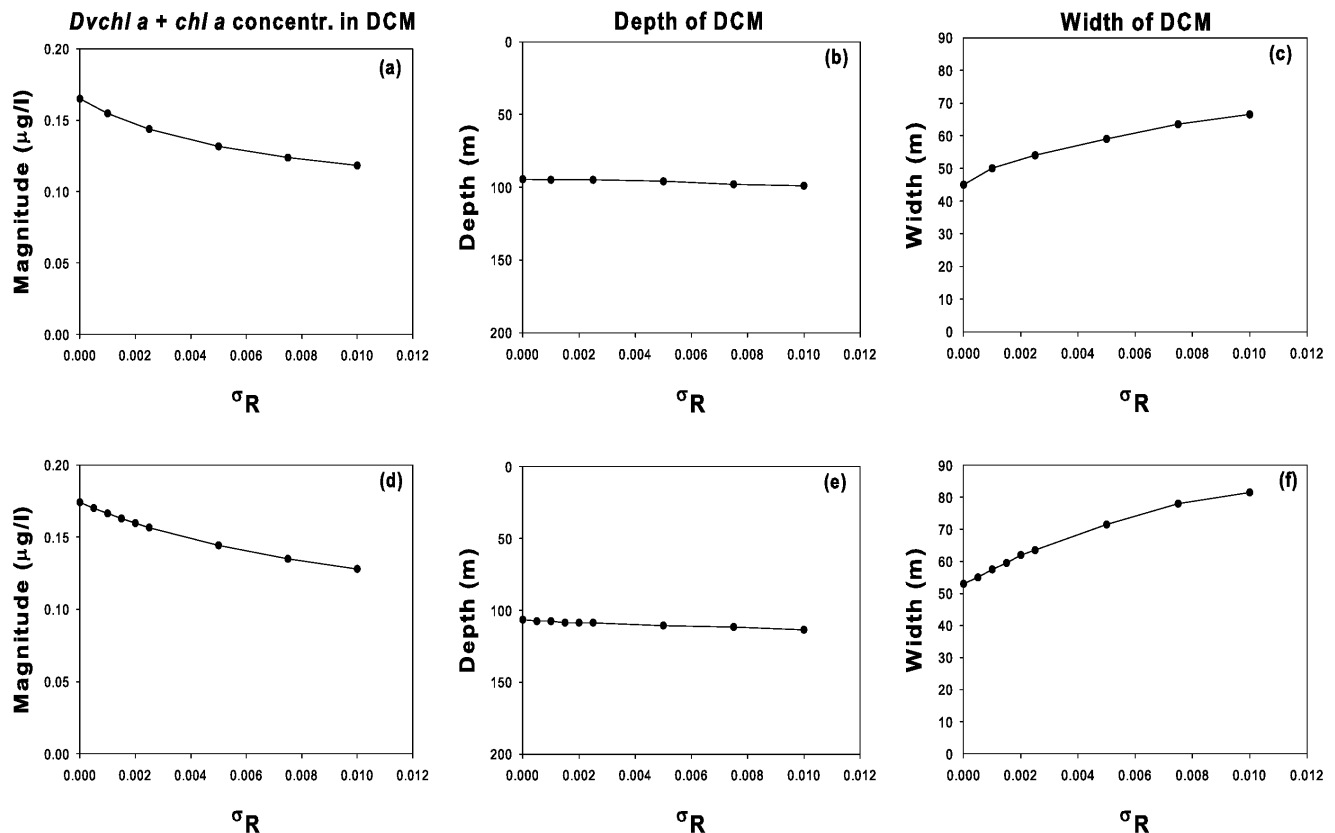


**Figure 9.** Magnitude, depth, and width of the DCM as a function of  $\sigma_R$  obtained from the model. The values were obtained in stationary regime for site L1129b (panels a, b, c) and site L1105 (panels d, e, f). doi:10.1371/journal.pone.0066765.g009

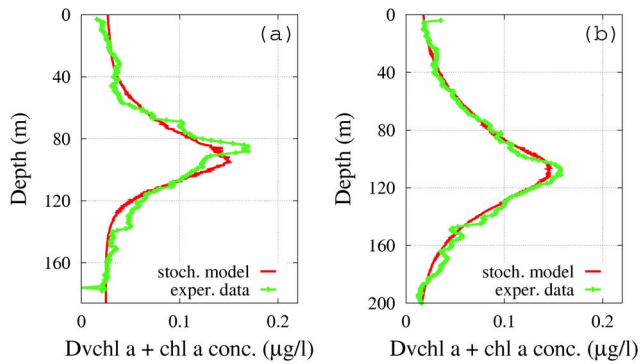


**Figure 10. Theoretical distributions (red line) of the total *chl a* and *Dvchl a* concentration (stochastic approach).** The profiles were obtained in stationary regime for a given set of noise intensities (case 2 of the stochastic model) as a function of depth, and are compared with the corresponding experimental distributions (green line) in sites L1129b (panel a) and L1105 (panel b). The theoretical values were obtained averaging over 1000 numerical realizations. The values of the parameters are those shown in Table 1. The noise intensities are: (a)  $\sigma_{b_1} = 0.22$ ,  $\sigma_{b_2} = 0.08$  and  $\sigma_R = 0.0025$  for site L1129b; (b)  $\sigma_{b_1} = 0.15$ ,  $\sigma_{b_2} = 0.10$  and  $\sigma_R = 0.0020$  for site L1105. (Color online). doi:10.1371/journal.pone.0066765.g010

nutrient competitor, i.e. *Prochlorococcus*. These results are in agreement with previous works of other authors [50,67].

In our model, we set in both sites the condition  $D \leq 3.0 \text{ cm}^2/\text{s}$ , corresponding to weakly mixed waters, which causes the phytoplankton peak to have a width of some meters, as observed in the experimental data. Furthermore, we fixed low values of the nutrient concentration at the bottom ( $R_{in} \leq 6.0 \text{ mmol nutrient m}^{-3}$ ), corresponding to the condition of oligotrophic waters in both sites. In general, for our set of parameters, the deep chlorophyll maximum is always formed by both groups, even if the peak of *Prochlorococcus* biomass is localized above DCM. It is important to underline that in our analysis we used along the water column a constant value of vertical turbulent diffusivity. However, in order to evaluate the effects of the presence of an upper mixed layer (UML), we analyzed the phytoplankton dynamics fixing, in the surface layers i.e. above the thermocline, a high value of vertical turbulent diffusivity ( $D = 50.0 \text{ cm}^2/\text{s}$ ). The numerical results (here not shown) were not in agreement with the experimental data. In conclusion, we observed that the approach used in Ref. [50,67] describes the mechanisms of our ecosystem better than the Yoshiyama approach [4,98].

In order to compare the numerical results with the experimental ones, we converted the theoretical biomass concentrations obtained from the model into *chl a* and *Dvchl a* concentration by using the mean vertical profile curves of Brunet et al. [51].

In our analysis, as a first step, we exploited a deterministic model. The results obtained show a qualitative agreement with the field observations, even if the theoretical and experimental distributions of total *chl a* and *Dvchl a* concentration present some differences. In particular, the shape of the numerical distribution of total *chl a* and *Dvchl a* concentration resulted quite different from the experimental profile in site L1129b, while the magnitude of the theoretical DCM in site L1105 was quite higher than the experimental value.

In order to take into account the effects of the noisy behaviour of the environmental variables, we inserted the contribution of the random fluctuations by adding a term of multiplicative Gaussian noise in the differential equation for the nutrient concentration (case 1). The numerical results showed that the presence of a noise source, which acts directly on the dynamics of the nutrient, allows to reproduce, in stationary conditions and for both marine sites analyzed, average profiles of the total *chl a* and *Dvchl a* concentration in a better agreement with the experimental findings respect to the deterministic case. In particular, on the basis of two comparative methods ( $\chi^2$  goodness-of-fit test and Kolmogorov-Smirnov test), we found that position, shape and magnitude of the DCMs agree very well with the experimental ones in both sites. Afterwards we modified the model, considering also the effects of two multiplicative Gaussian noise sources, which act directly on the two picophytoplankton groups (case 2). In these conditions, for suitable noise intensities, the  $\chi^2$  goodness-of-fit test exhibit in both sites values much lower than those previously obtained by the stochastic model in case 1. Viceversa, the values obtained from the Kolmogorov-Smirnov test became worse respect to the deterministic model in one of the two marine sites analyzed, but remained unaltered for the other site, indicating that the random fluctuations which affect the nutrient dynamics play a main role in the dynamics of the ecosystem.

## Conclusions

The results presented show that the stochastic model, which considers the dynamics of picoeukaryotes and *Prochlorococcus*, is able to reproduce biomass distributions in a marine ecosystem characterized by weakly mixed waters. In particular this work presents two novelties. First, a stochastic approach is used to describe the dynamics of two picophytoplankton populations. Second, theoretical results for biomass concentrations are converted into the corresponding chlorophyll content. This allows to perform a direct comparison between the chlorophyll concentration obtained by the model and the same quantity sampled in two different marine sites. A good agreement between theoretical results and experimental findings is obtained thanks to the presence of both phytoplankton groups considered in our analysis. More specifically, the approach used in this work allows to get distributions of total *chl a* and *Dvchl a* concentration in a good

**Table 4. Results of  $\chi^2$ , reduced chi-square ( $\tilde{\chi}^2$ ), and Kolmogorov-Smirnov goodness-of-fit tests for sites L1129b and L1105, at fixed values of  $\sigma_{b_1}$ ,  $\sigma_{b_2}$  and  $\sigma_R$  (stochastic dynamics - case 2).**

Site	$R_{in}$	$\sigma_R$	$\sigma_{b_1}$	$\sigma_{b_2}$	$\chi^2$	$\tilde{\chi}^2$	D (K-S)	P (K-S)
L1129b	5	0.0025	0.22	0.08	0.33	0.0019	0.1136	0.193
L1105	6	0.0020	0.15	0.10	0.16	0.0008	0.0914	0.3670

D(K-S) and P(K-S) are the maximum difference between the cumulative distributions and the corresponding probability for the K-S test, respectively. The number of samples, used for the tests and distanced of 1 m, is  $n = 176$  for site L1129b, corresponding to consider the whole water column, and  $n = 200$  for site L1105, corresponding to consider from the surface the first 200 m of depth.

doi:10.1371/journal.pone.0066765.t004

agreement with the experimental ones, even if the equations do not include explicitly environmental variables such as salinity, temperature and velocity field. We conclude observing that the results of this work could contribute, within the context of aquatic ecosystems, to devise a new class of models based on a stochastic approach and able to predict future changes, produced by global warming, in phytoplankton distributions.

## References

- Mann KH, Lazier JRN (1996) Dynamics of marine ecosystems. Malden, MA, USA: Blackwell Publishing.
- Klausmeier CA, Litchman E (2001) Algal games: the vertical distribution of phytoplankton in poorly mixed water columns. *Limnol Oceanogr* 46: 1998–2007.
- Huisman J, Thi NPT, Karl DM, Sommeijer B (2006) Reduced mixing generates oscillations and chaos in the oceanic deep chlorophyll maximum. *Nature* 439: 322–325.
- Ryabov AB, Rudolf L, Blasius B (2010) Vertical distribution and composition of phytoplankton under the influence of an upper mixed layer. *J Theor Biol* 263: 120–133.
- Hickman A, Dutkiewicz S, Williams R, Follows M (2010) Modelling the effects of chromatic adaptation on phytoplankton community structure in the oligotrophic ocean. *Mar Ecol Prog Ser* 406: 1–17.
- Beverdoff L, Miller T, McMahon K (2013) The role of nitrogen fixation in cyanobacterial bloom toxicity in a temperate, eutrophic lake. *PLoS ONE* 8(2): e56103.
- Grenfell BT, Wilson K, Finkenstädt BF, Coulson TN, Murray S, et al. (1998) Noise and determinism in synchronized sheep dynamics. *Nature* 394: 674–677.
- Zimmer C (1999) Life after chaos. *Science* 284: 83–86.
- Bjornstad ON, Grenfell BT (2001) Noisy clockwork: Time series analysis of population fluctuations in animals. *Science* 293: 638–643.
- Spagnolo B, Cirone M, La Barbera A, de Pasquale F (2002) Noise induced effects in population dynamics. *J Phys* 14: 2247–2255.
- La Barbera A, Spagnolo B (2002) Spatio-temporal patterns in population dynamics. *Physica A* 314: 120–124.
- Spagnolo B, La Barbera A (2002) Role of the noise on the transient dynamics of an ecosystem of interacting species. *Physica A* 315: 114–124.
- Spagnolo B, Fiasconaro A, Valenti D (2003) Noise induced phenomena in Lotka-Volterra systems. *Fluct Noise Lett* 3: L177–L185.
- Spagnolo B, Valenti D, Fiasconaro A (2004) Noise in ecosystems: A short review. *Math Biosci Eng* 1: 185–211.
- Valenti D, Fiasconaro A, Spagnolo B (2004) Pattern formation and spatial correlation induced by the noise in two competing species. *Acta Phys Pol B* 35: 1481–1489.
- Spagnolo B, Valenti D, Fiasconaro A (2005) Transient behavior of a population dynamical model. *Prog Theor Phys Supp* 157: 312–316.
- Caruso A, Gargano ME, Valenti D, Fiasconaro A, Spagnolo B (2005) Cyclic fluctuations, climatic changes and role of noise in planktonic foraminifera in the Mediterranean Sea. *Fluct Noise Lett* 5: L349–L355.
- Chichigina O, Valenti D, Spagnolo B (2005) A simple noise model with memory for biological systems. *Fluct Noise Lett* 5: L243–L250.
- Fiasconaro A, Valenti D, Spagnolo B (2006) Asymptotic regime in N random interacting species. *Eur Phys J B* 50: 189–194.
- Valenti D, Schimansky-Geier L, Sailer X, Spagnolo B (2006) Moment equations for a spatially extended system of two competing species. *Eur Phys J B* 50: 199–203.
- Chichigina OA (2008) Noise with memory as a model of lemming cycles. *Eur Phys J B* 65: 347–352.
- La Cognata A, Valenti D, Dubkov A, Spagnolo B (2010) Dynamics of two competing species in the presence of levy noise sources. *Phys Rev E* 81: 011121(1–8).
- Chichigina OA, Dubkov AA, Valenti D, Spagnolo B (2011) Stability in a system subject to noise with regulated periodicity. *Phys Rev E* 84: 021134(1–10).
- Goryachev A, Toh DJ, Wee KB, Lee T, Zhang HB, et al. (2005) Transition to quorum sensing in an agrobacterium population: A stochastic model. *PLoS Comput Biol* 1(4): e37.
- Maye A, Hsieh CH, Sugihara G, Brembs B (2007) Order in spontaneous behavior. *PLoS ONE* 2(5): e443.
- Valenti D, Spagnolo B, Bonanno G (2007) Hitting time distributions in financial markets. *Physica A* 382: 311–320.
- Valenti D, Denaro G, La Cognata A, Spagnolo B, Bonanno A, et al. (2012) Picophytoplankton dynamics in noisy marine environment. *Acta Phys Pol B* 43: 1227–1240.
- Denaro G, Valenti D, La Cognata A, Spagnolo B, Bonanno A, et al. (2013) Spatio-temporal behaviour of the deep chlorophyll maximum in mediterranean

## Acknowledgments

We thank Prof. Dr. Lutz Schimansky-Geier and Dr. Christophe Brunet for advice and useful discussions.

## Author Contributions

Conceived and designed the experiments: GB SM SWZ SA AB. Performed the experiments: GB SM SWZ SA AB. Analyzed the data: GD DV BS. Contributed reagents/materials/analysis tools: GB SM SWZ SA AB. Wrote the paper: GD DV BS. Designed the software used to solve numerically the equations of the system: GD.

- Development of a stochastic model for picophytoplankton dynamics. *Ecol Complex* 13: 21–34.
- Veldhuis MJW, Timmermans KR, Croot P, Van Der Wagt B (2005) Picophytoplankton; a comparative study of their biochemical composition and photosynthetic properties. *J Sea Res* 53: 7–24.
- Karsenti E, Acinas S, Bork P, Bowler C, Vargas CD, et al. (2011) A holistic approach to marine eco-systems biology. *PLoS Biol* 9(10): e1001177.
- Li WKW (1995) Composition of ultraphytoplankton in the central North Atlantic. *Mar Ecol Prog Ser* 122: 1–8.
- Estrada M (1996) Primary production in the North-Western Mediterranean. *Sci Mar* 60: 5564.
- Mei ZP, Finkel ZV, Irwin AJ (2009) Light and nutrient availability affect the size-scaling of growth in phytoplankton. *J Theor Biol* 259: 582–588.
- Patti B, Guisande C, Bonanno A, Basilone G, Cuttitta A, et al. (2010) Role of physical forcings and nutrient availability on the control of satellite-based chlorophyll a concentration in the coastal upwelling area of the Sicilian Channel. *Sci Mar* 74(3).
- Behrenfeld M, O'Malley R, Siegel D, McClain C, Sarmiento J, et al. (2006) Climate-driven trends in contemporary ocean productivity. *Nature* 444.
- Barale V, Jaquet JM, Ndiaye M (2008) Algal blooming patterns and anomalies in the Mediteranean Sea as derived from the SeaWiFS data set (1998–2003). *Remote Sens Environ* 112: 3300–3313.
- Cuttitta A, Carini V, Patti B, Bonanno A, Basilone G, et al. (2003) Anchovy egg and larval distribution in relation to biological and physical oceanography in the Strait of Sicily. *Hydrobiologia* 503: 117–120.
- Weston K, Fernand L, Mills DK, Delahunty R, Brown J (2005) Primary production in the deep chlorophyll maximum of the central North Sea. *J Plankton Res* 27: 909–922.
- Melbourne-Thomas J, Constable A, Wotherspoon S, Raymond B (2013) Testing paradigms of ecosystem change under climate warming in antarctica. *PLoS ONE* 8(2): e55093.
- Basilone G, Guisande C, Patti B, Mazzola S, Cuttitta A, et al. (2004) Linking habitat conditions and growth in the european anchovy (*Engraulis encrasicolus*). *Fish Res* 68: 9–19.
- Klausmeier CA, Litchman E, Levin SA (2007) A model of flexible uptake of two essential resources. *J Theor Biol* 246: 278–289.
- Thingstad TF, Rassoulzadegan F (1995) Nutrient limitations, microbial food webs, and biological C-pumps: suggested interactions in a P-limited Mediterranean. *Mar Ecol Prog Ser* 117: 299306.
- Ribera d'Alcalá M, Civitarese G, Conversano F, Lavezza R (2003) Nutrient ratios and fluxes hint at overlooked processes in the Mediterranean Sea. *J Geophys Res* 108.
- Norberg J (2004) Biodiversity and ecosystem functioning: a complex adaptive systems approach. *Limnol Oceanogr* 49: 1269–1277.
- Yeo SK, Huggett M, Eiler A, Rappé M (2013) Coastal bacterioplankton community dynamics in response to a natural disturbance. *PLoS ONE* 8(2): e56207.
- Fogg GE (1991) The phytoplanktonic ways of life. *New Phytol* 118: 191–232.
- Prézelin BB, Tilzer MM, Schofield O, Haese C (1991) The control of the production process of phytoplankton by the physical structure of the aquatic environment with special reference to its optical properties. *Aquat Sci* 53: 136–186.
- Brunet C, Casotti R, Vantrepotte V, Corato F, Conversano F (2006) Picophytoplankton diversity and photoacclimation in the Strait of Sicily (Mediterranean Sea) in summer. I. Mesoscale variations. *Aquat Microb Ecol* 44: 127–141.
- Garczarek L, Dufresne A, Rousvoal S, West NJ, Mazard S, et al. (2007) High vertical and low horizontal diversity of prochlorococcus ecotypes in the Mediterranean Sea in summer. *FEMS Microbiol Ecol* 60: 189–206.
- Ryabov A (2012) Phytoplankton competition in deep biomass maximum. *Theor Ecol* 5: 373–385.
- Brunet C, Casotti R, Vantrepotte V, Conversano F (2007) Vertical variability and diel dynamics of picophytoplankton in the Strait of Sicily, Mediterranean Sea, in summer. *Mar Ecol Prog Ser* 346: 15–26.
- Casotti R, Brunet C, Aronne B, Ribera d'Alcalá M (2000) Mesoscale features of phytoplankton and planktonic bacteria in a coastal area as induced by external water masses. *Mar Ecol Prog Ser* 195: 15–27.



53. Casotti R, Landolfi A, Brunet C, D'Ortenzio F, Mangoni O, et al. (2003) Composition and dynamics of the phytoplankton of the Ionian Sea (Eastern Mediterranean). *J Geophys Res* 108.
54. Raven JA, Finkel ZV, Irwin AJ (2005) Picophytoplankton: bottom-up and top-down controls on ecology and evolution. *J Geophys Res* 55: 209–205.
55. Dimier C, Corato F, Saviello G, Brunet C (2007) Photophysiological properties of the marine picoeukaryotes *picochlorum rcc 237* (Trebouxiophyceae chlorophyta). *J Phycol* 43: 275–283.
56. Worden AZ, Not F (2008) *Microbial Ecology of the Oceans*, Second Edition. John Wiley & Sons, Inc.
57. Mendonça A, Aristegui J, Vilas J, Montero M, Ojeda A, et al. (2012) Is there a seamount effect on microbial community structure and biomass? The case study of Seine and Sedlo Seamounts (Northeast Atlantic). *PLoS ONE* 7(1): e29526.
58. Raven JA (1998) The twelfth tansley lecture. small is beautiful: The picophytoplankton. *Funct Ecol* 12: 503.
59. Brunet C, Casotti R, Aronne B, Vantrepotte V (2003) Measured photophysiological parameters used as tools to estimate vertical water movements in the coastal Mediterranean. *J Plankton Res* 25: 1413–1425.
60. Finkel ZV, Irwin AJ (2005) Picophytoplankton: Bottom-up and top-down controls on ecology and evolution. *Vie Milieu* 55: 209–215.
61. Brunet C, Casotti R, Vantrepotte V (2008) Phytoplankton diel and vertical variability in photo-biological responses at a coastal station in the Mediterranean Sea. *J Plankton Res* 30: 645–654.
62. Dimier C, Saviello G, Tramontano F, Brunet C (2009) Comparative ecophysiology of the xantho-phyll cycle in six marine phytoplanktonic species. *Protist* 160: 397–411.
63. Moore LR, Goericke R, Chisholm SW (1995) Comparative physiology of synechococcus and prochlorococcus: influence of light and temperature on growth, pigments, fluorescence and absorptive properties. *Mar Ecol Prog Ser* 116: 259–275.
64. Partensky F, Hess W, Vaulot D (1999) Prochlorococcus, a marine photosynthetic prokaryote of global significance. *Microbiol Mol Biol R* 63: 106–127.
65. Bougaran G, Bernard O, Sciandra A (2010) Modeling continuous cultures of microalgae colimited by nitrogen and phosphorus. *J Theor Biol* 265: 443454.
66. Turpin DH (1988) Physiological mechanisms in phytoplankton resource competition (316–368). In: *Growth and reproductive strategies of freshwater phytoplankton*. Cambridge University Press.
67. Ryabov A, Blasius B (2011) A graphical theory of competition on spatial resource gradients. *Ecol Lett* 14: 220–228.
68. Shigesada N, Okubo A (1981) Effects of competition and shading in planktonic communities. *J Math Biol* 12: 311–326.
69. Kirk JTO (1994) *Light and Photosynthesis in Aquatic Ecosystems* (2nd edition). Cambridge University Press.
70. Valenti D, Fiasconaro A, Spagnolo B (2004) Stochastic resonance and noise delayed extinction in a model of two competing species. *Physica A* 331: 477–486.
71. Huppert A, Blasius B, Olinky R, Stone L (2005) A model for seasonal phytoplankton blooms. *J Theor Biol* 236: 276–290.
72. Ebeling W, Spagnolo B (2005) Noise in condensed matter and complex systems. *Fluct Noise Lett* 5: L159–L161.
73. Liu QX, Jin Z, Li BL (2008) Resonance and frequency-locking phenomena in spatially extended phytoplankton-zooplankton system with additive noise and periodic forces. *J Stat Mech-Theory E* 2008.
74. Provata A, Sokolov I, Spagnolo B (2008) Editorial: Ecological complex systems. *Eur Phys J B* 65: 307–314.
75. Spagnolo B, Dubkov AA (2008) Editorial of critical phenomena and diffusion in complex systems. *Int J Bifurcat Chaos* 18: 2643–2647.
76. Valenti D, Tranchina L, Cosentino C, Brai M, Caruso A, et al. (2008) Environmental metal pollution considered as noise: Effects on the spatial distribution of benthic foraminifera in two coastal marine areas of Sicily (Southern Italy). *Ecol Model* 213: 449–462.
77. Spagnolo B, Spezia S, Curcio L, Pizzolato N, Fiasconaro A, et al. (2009) Noise effects in two different biological systems. *Eur Phys J B* 69: 133–146.
78. Mikhailov AS, Loskutov AY (1996) *Foundations of Synergetics II: Chaos and Noise*. Springer Series in Synergetics. Springer, Berlin.
79. Muñoz MA, Colaioni F, Castellano C (2005) Mean-field limit of systems with multiplicative noise. *Phys Rev E* 72: 056102.
80. Manor A, Shnerb N (2009) Multiplicative noise and second order phase transitions. *Phys Rev Lett* 103: 030601.
81. Schenzle A, Brand H (1979) Multiplicative stochastic processes in statistical physics. *Phys Rev A* 20: 1628–1647.
82. Graham R, Schenzle A (1982) Carleman imbedding of multiplicative stochastic processes. *Phys Rev A* 25: 1731–1754.
83. García-Ojalvo J, Sancho JM (1999) *Noise in Spatially Extended Systems*. Springer, New York.
84. Redner S (1990) Random multiplicative processes: An elementary tutorial. *Am J Phys* 58: 267–273.
85. Sornette D (2000) *Critical Phenomena in Natural Sciences*. Springer Series in Synergetics. Springer, Heidelberg.
86. Barrera P, Ciuchi S, Spagnolo B (1993) Generating function for a multiplicative noise with group analysis. *J Phys A: Math Gen* 26: L559–L565.
87. Ciuchi S, de Pasquale F, Spagnolo B (1993) Nonlinear relaxation in the presence of an absorbing barrier. *Phys Rev E* 47: 3915–3926.
88. Ciuchi S, de Pasquale F, Spagnolo B (1996) Self-regulation mechanism of an ecosystem in a non-gaussian fluctuation regime. *Phys Rev E* 54: 706–716.
89. Dimier C, Brunet C, Geider R, Raven J (2009) Growth and photoregulation dynamics of the picoeukaryote *Pelagomonas calceolata* in fluctuating light. *Limnol Oceanogr* 54: 823–836.
90. Moon-Van Der Staay SY, De Wachter R, Vaulot D (2001) Oceanic 18S rDNA sequences from picoplankton reveal unsuspected eukaryotic diversity. *Nature* 409: 607–610.
91. Fennel K, Boss E (2003) Subsurface maxima of phytoplankton and chlorophyll: Steady-state solutions from a simple model. *Limnol Oceanogr* 48: 1521–1534.
92. Horsthemke W, Lefever R (1984) *Noise-Induced Transitions: Theory and Applications in Physics, Chemistry, and Biology*. Springer-Verlag, Berlin Heidelberg.
93. Brunet C, Lavaud J (2010) Can the xanthophyll cycle help extract the essence of the microalgal functional response to a variable light environment? *J Plankton Res* 32: 1609–1617.
94. Giuffrida A, Valenti D, Ziino G, Spagnolo B, Panebianco A (2009) A stochastic interspecific competition model to predict the behaviour of *Listeria monocytogenes* in the fermentation process of a traditional sicilian salami. *Eur Food Res Technol* 228.
95. Bibby TS, Mary I, Nield J, Partensky F, Barber J (2003) Low light adapted prochlorococcus species possess specific antennae for each photosystem. *Nature* 424: 1051–1054.
96. Moore LR, Rocap G, Chisholm SW (1998) Physiology and molecular phylogeny of coexisting Prochlorococcus ecotypes. *Nature* 397: 464–467.
97. Huisman J, Sharples J, Stroom JM, Visser PM, Kardinaal WEN, et al. (2004) Changes in turbulent mixing shift competition for light between phytoplankton species. *Ecology* 85: 2960–2970.
98. Yoshiyama K, Mellard J, Litchman E, Klausmeier C (2009) Phytoplankton competition for nutrients and light in a stratified water column. *Am Nat* 174.
99. Rippka R, Coursin T, Hess W, Lichtle C, Scanlan DJ, et al. (2000) *Prochlorococcus marinus* Chisholm et al. 1992 subsp. *pastoris* subsp. nov. strain PCC 9511, the first axenic chlorophyll *a2/b2*-containing cyanobacterium (Oxyphotobacteria). *Int J Syst Evol Micr* 50: 1833–1847.
100. Denaro G, Valenti D, Spagnolo B, Bonanno A, Basilone G, et al. (2013) Stochastic Dynamics of Two Picophytoplankton Populations in a Real Marine Ecosystem. *Acta Phys. Pol. B* 44: 977–990. In press. DOI:10.5506/APhysPolB.44.977.